Two-dimensional cluster-state preparation with linear ion traps

Harald Wunderlich* and Christof Wunderlich†
Fachbereich Physik, Universität Siegen, 57068 Siegen, Germany

Kilian Singer and Ferdinand Schmidt-Kaler
Universität Ulm, Institut für Quanteninformationsverarbeitung, Albert-Einstein-Allee 11, 89069 Ulm, Germany
(Dated: October 30, 2018)

We present schemes to prepare two-dimensional cluster states [H. J. Briegel and R. Raussendorf, Phys. Rev. Lett. **86**, 910 (2001)] with atomic ions confined in a microstructured linear ion trap and coupled by an engineered spin-spin interaction. In particular, we show how to prepare a $n \times 2$ cluster state by creating a linear cluster state and adding third-neighbor entanglement using selective recoupling techniques. The scheme is based on the capabilities provided by segmented linear Paul traps to confine ions in local potential wells and to separate and transport ions between these wells. Furthermore, we consider creating three- and four-qubit cluster states by engineering the coupling matrix such that through the periodicity of the time evolution unwanted couplings are canceled. All entangling operations are achieved by switching of voltages and currents, and do not require interaction with laser light.

PACS numbers: 03.67.Bg, 03.67.Lx, 37.10.Ty

I. INTRODUCTION

Cluster states [1] are the physical resource needed for a one-way quantum computer [2, 3] – a scheme for measurement-based quantum computation [4]. It has been shown that the one-way quantum computer provides a universal set of quantum gates. Furthermore, cluster states can be used to efficiently simulate quantum circuits. On the other hand, some quantum circuits based on the cluster-state model cannot be interpreted as a network of gates such as the bit-reversal gate [5].

Not only are cluster states a central ingredient for measurement-based quantum computing, they are also of interest for investigating questions of fundamental relevance, for instance, regarding the robustness of entanglement. The presumption that the lifetime of entanglement decreases with the number of constituents of an entangled system and that, therefore, entanglement does not have to be taken into account when describing the properties of mesoscopic and macroscopic systems is widespread. This is indeed true, for example, for Greenberger-Horne-Zeilinger [6] states for which the decoherence rate increases linearly with the number N of qubits. However, such behavior does not necessarily hold for other N-particle systems. In fact, many-body states exist where the entanglement between the constituents is expected to not decay faster than that determined by the decoherence rate of a single qubit [7]. Cluster states belong to this class of entangled states.

The topology of cluster states may exist in different dimensions. In [8] it is shown that one-dimensional (1D) cluster states can be efficiently simulated by classical computers, thus two-dimensional (2D) cluster states are needed for useful quantum computation. The first experimental realization of cluster states was reported in [9]. In that experiment, the entanglement was created using controlled collisions between atoms confined in an optical lattice. Photonic one-way quantum computers have already been used to implement quantum algorithms, namely, Grover's algorithm [10] and the Deutsch algorithm on a four-photon cluster state [11]. Four- and six-qubit cluster states have also been recently experimentally realized with photons [12, 13].

Until now, multi-qubit cluster states have not been created with trapped ions. In [14] it was proposed to generate a linear cluster state of four, five, and six ions in a linear Paul trap using a gate similar to the Mølmer-Sørenson gate [15, 16]. This would be accomplished by collective addressing of all ions by means of two laser beams tuned to the blue- and red-sideband transition of the exploited vibrational mode. This technique is robust against heating and does not require the ions to be cooled into their motional ground state. However, scaling this method to larger numbers of ions becomes complex.

In this paper we propose schemes to prepare two-dimensional cluster states with atomic ions confined in a linear (one-dimensional) trap. In contrast to the scheme described above, we consider creating cluster states by means of spin-spin coupling induced by a magnetic-field gradient that creates a state-dependent force acting on each qubit. Here, laser light is not required to achieve an entangling gate between the ions. Furthermore, we consider two-dimensional cluster states, and suggest that our scheme should be highly scalable. In addition, cooling the ion string to its motional ground is not necessary.

An easily scalable method for preparing cluster states is applying a Hamiltonian equivalent to an Ising-type interaction on qubits, initially prepared in states $|+\rangle =$

*Electronic address: h.wunderlich@physik.uni-siegen.de
†Electronic address: wunderlich@physik.uni-siegen.de

$\frac{1}{\sqrt{2}}(|0\rangle + |1\rangle)$ [1]:

$$H = \hbar \sum_{a,a'} J_{a,a'} \frac{1+\sigma_z^{(a)}}{2} \frac{1-\sigma_z^{(a')}}{2} \qquad (1)$$

The time evolution $e^{-iHt/\hbar}|+\rangle^{\otimes^n}$ results in cluster states, if $J_{a,a'}t = \pi + 2k\pi$ with $k \in \mathbb{N}$ and restricting the interaction to next neighbors yields two-dimensional cluster states. However, in general, experimentally accessible J couplings $J_{a,a'}$ are of such a form that preparing cluster states (or performing other operations) is not trivial.

This paper presents methods to engineer spin-spin couplings suitable for generating two-dimensional cluster states, a prerequisite for one-way quantum computing with state-of-the-art linear ion traps. The outline of the paper is as follows: Sec. I A is a review of how one-way computing with two-dimensional cluster states can be implemented on a smaller number of physical qubits by reusing those qubits that have been measured during the computational process.

In Sec. I B we summarize the relevant properties of a collection of spin-coupled trapped ions and then explicitly show in Sec. II how to prepare a $n \times 2$ cluster state with a number of operational steps that is linear in n using this system.

Section II A deals with schemes for cluster state generation, where the local electrostatic trapping potential experienced by each ion is individually adjustable. We outline two schemes that are primarily suited for creating one-dimensional cluster states, even though they could, in principle, be used to generate two-dimensional clusters. For implementing the first scheme, proposed by Mc Hugh and Twamley [17, 18], the harmonic oscillator frequencies that characterize the local trapping potentials are set to equal values, resulting in uniform nearest neighbor couplings. Controlled generation of nearest neighbor couplings by a choice of appropriate non-uniform trap frequencies is considered in the second scheme. Then, with the help of numerical simulations based on an existing microstructured ion trap, we show that these methods require smaller trap-electrode structures than currently available to attain coupling constants that are useful in practice for cluster state generation.

While the above mentioned schemes are based on nearest-neighbor interactions provided by individual potential wells, Sec. II A 2 deals with the question of whether coupling constants can be engineered in such a way that they fulfill periodicity conditions imposed on the time-evolution operator suitable for generating cluster states in one time-evolution step.

In Sec. II B we propose a scalable scheme for creating two-dimensional cluster states, which does not rely on a static placement of the ions in individual wells. Instead it makes use of the possibilities provided by segmented traps to adiabatically transport ions, and separate ions held in common traps, thus allowing us to circumvent problems arising in the previously mentioned schemes.

The scheme for creating 2D cluster states detailed in Secs. II A and II B is underpinned by simulations of electrostatic potentials in a microstructured ion trap. To be concrete, we used for this purpose the parameters of a microtrap that is currently being developed.

A. Breaking up a $n \times m$ cluster state into clusters of size $n \times 2$

In order to make one-way quantum computing possible first a two-dimensional $n \times m$ cluster state needs to be prepared and then single-qubit adaptive measurements in qubit-specific bases are performed in order to achieve a quantum gate [3]. The basis of a measurement may depend on the outcome of previous measurements.

The question this paper deals with is: "How can a two-dimensional cluster-state be efficiently prepared with trapped ions?" Generally, preparing a two-dimensional cluster-state turns out to be difficult for an arbitrary number of qubits. In order to work out an experimentally feasible procedure for generating cluster states, we notice that - within the scope of the one-way model - a $n \times m$ cluster state may be broken up into segments of dimension $n \times 2$ as shown by Mc Hugh [17] and recapitulated for the reader's convenience in what follows.

The usual way to implement a measurement based quantum computer is to prepare the entangled state followed by single-qubit measurements. This procedure is equivalent to the following: imagine the qubits arranged in a two-dimensional array. Then, the initial state containing the input data for the quantum gate to be performed is written upon the first column of qubits. The second column is prepared in the state $|+\rangle = \frac{1}{\sqrt{2}}(|0\rangle + |1\rangle)$. After entangling all qubits with their nearest neighbors via the time evolution generated by Hamiltonian (1) with $J_{a,a'}t = \pi$, a $n \times 2$ cluster state is established. Now, measurements on the first column are performed in a predetermined basis such that these measurements amount to executing a desired quantum gate. Due to the entanglement, the quantum information generated by these measurements is thus transferred to the second column's qubits. At the same time, the entanglement between the two columns is erased by the measurement operation.

That means, the first column may now be used to simulate the third column of a $n \times m$ cluster. For this purpose, its qubits are prepared in the state $|+\rangle$ and entangled with the second column's qubits. Then, single-qubit measurements are performed on the second column so that the quantum information is transferred to the first column's qubits. Thus, performing this procedure $m-1$ times, one can simulate a $n \times m$ cluster via a $n \times 2$ cluster.

B. Spin-coupled trapped ions

We consider N ions of mass m confined strongly in two spatial dimensions (x and y direction) and by a weaker potential in the third (z direction). This can be achieved, for example, by using a linear electrodynamic trap where the effective harmonic confinement in the radial direction, measured in terms of the secular angular frequency ν_r, is much stronger than in the axial direction characterized by secular frequency ν_z [19, 20, 21]. The ions are laser cooled such that their radial degrees of freedom are frozen out and they form a linear Coulomb crystal.

Each ion provides two internal levels (e.g., hyperfine states) serving as qubits described by the Pauli operator σ_z. In addition, a magnetic field $\vec{B} = (B_0 + bz)\vec{e}_z$ is applied such that the ions experience a gradient b along the z-axis. Then, the Hamiltonian of the system reads [18, 22, 23]:

$$H = \frac{\hbar}{2}\sum_{n=1}^{N}\omega_n(z_{0,n})\sigma_{z,n} + \sum_{n=1}^{N}\hbar\nu_n a_n^\dagger a_n - \frac{\hbar}{2}\sum_{n<m}J_{nm}\sigma_{z,n}\sigma_{z,m}. \tag{2}$$

The first term of the Hamiltonian represents the internal energies of N qubits where the qubit resonances are given by $\omega_n(z_{0,n})$, and $z_{0,n}$ is the axial equilibrium position of the nth ion. The second term expresses the collective quantized vibrational motion in the axial direction of the ions with eigenfrequency ν_n of vibrational eigenmode n. The last term describes a pairwise spin-spin coupling between qubits with the coupling constants.

$$\begin{aligned} J_{nm} &= \frac{\hbar}{2m}\sum_{j=1}^{N}\frac{1}{\nu_j^2}\frac{\partial\omega_n}{\partial z_n}|_{z_{0,n}}\frac{\partial\omega_m}{\partial z_m}|_{z_{0,m}}D_{nj}D_{mj} \\ &= \frac{\hbar}{2}\frac{\partial\omega_n}{\partial z_n}|_{z_{0,n}}\frac{\partial\omega_m}{\partial z_m}|_{z_{0,m}}(A^{-1})_{nm}, \end{aligned} \tag{3}$$

where A is the Hessian of the trap potential and D is the unitary transformation matrix that diagonalizes A. The eigenvalues of A are given by $m\nu_j^2$. Therefore, the spin chain can be interpreted as an N-qubit molecule with adjustable coupling constants J_{nm}, an ion spin molecule. If the ions are confined in a global harmonic potential, then $J_{nm} \propto b^2/\nu_1^2$.

In Fig. 1, as a concrete example, the coupling constants J_{nm} are displayed for eight $^{171}\mathrm{Yb}^+$ions in a linear trap characterized by $\nu_1 = 2\pi \cdot 200\,\mathrm{kHz}$ and a magnetic field gradient of $100\,\mathrm{T/m}$.

So far we have a considered a global axial potential confining the ion string. However, the trapping potential for each ion may be shaped such that the ions reside in individual harmonic potential wells. This is accomplished by dividing the dc electrode of a linear Paul trap into segments to which individual voltages may be applied that shape the axial potential experienced by the ions. Thus, one or more ions may be held in local potential wells, and there are additional handles to change the range and strength of the coupling constants J_{nm} [18]. Recently, segmented microstructured traps have been investigated experimentally and theoretically. Such traps provide the capability of storing ions in separate potential wells, and of separating and transporting ions into different trap regions [24, 25, 26, 27, 28, 29].

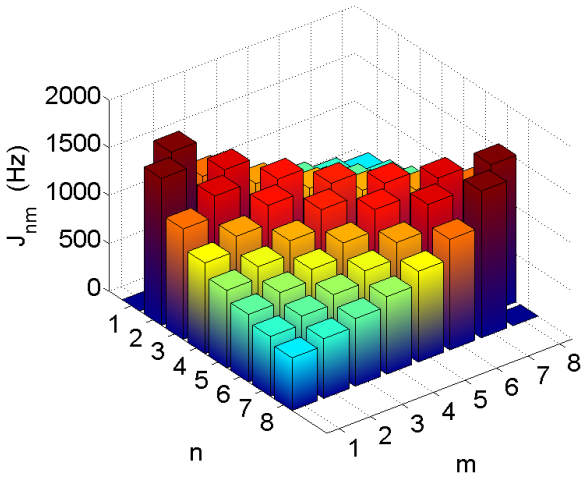

FIG. 1: (Color online) Coupling constants for eight Yb^+ ions in a Paul trap with axial trap frequency $\nu_1 = 2\pi \times 200\,\mathrm{kHz}$ and a magnetic field gradient of $100\,\mathrm{T/m}$.

The spin-spin coupling mediated by the vibrational motion in Eq. (2) arises when the ions are exposed to a magnetic field gradient that induces a state-dependent force. The scheme for cluster-state preparation proposed here can also be applied to the case when the required spin-spin coupling is generated by means other than a magnetic-field gradient. In [30] it was shown that an optical state-dependent force may induce a coupling whose formal description is identical to what is outlined above. Electrons confined in an array of microstructured Penning traps and exposed to a spatially varying magnetic field also exhibit a similar spin-spin coupling [31, 32, 33].

II. PREPARING CLUSTER STATES USING SPIN-SPIN INTERACTIONS

Spin-spin coupling as it appears in Eq. (2) may be used to prepare cluster states. This is achieved in two steps [1]: first, all qubits are prepared in the state $|+\rangle$. Second, the spin-spin coupling according to Eq. (2) is switched on for a time such that $\int J_{nm}dt = \frac{\pi}{2} + 2k\pi$, $k \in \mathbb{N}$ for all qubit pairs (n, m) that are to be entangled. This way of preparing cluster states provides, in principle, an efficient and scalable method to generate entangled states.

In actual experiments, the above condition can be ful-

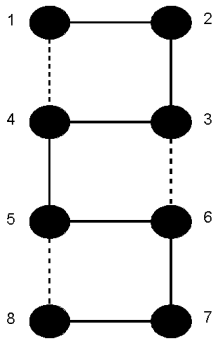

FIG. 2: Preparing a 4×2 cluster-state: In a first sequence of operations, a linear 8-qubit cluster-state is created (indicated by solid lines connecting the qubits). The second sequence then yields entanglement of third-neighbor qubits (dashed lines) resulting in the two-dimensional cluster topology.

filled by manipulating the coupling constants, by applying a pulse sequence to selectively realize specific couplings, or by combining these two methods. In what follows, we will address the issue of creating suitable interactions for cluster state preparation in detail.

With a string of trapped ions, if all ions are located in the same harmonic potential well, the J couplings vary in strength throughout the ion string (see Fig. 1). Thus, achieving controlled dynamics of the system is possible only at high cost, for example by using selective recoupling pulse sequences whose length grows quadratically with the qubit number [34]. Furthermore, the vibrational motion of the ion string is mediated by the Coulomb repulsion. So J couplings decrease for non-nearest neighbors. This turns out to be a serious problem for an efficient preparation of large two-dimensional cluster-states.

The coarse procedure for creating $n \times 2$ cluster states that forms the basis for the schemes presented in the remainder of this paper (unless noted otherwise as in Sec. II A 2) is illustrated in Fig. 2. First, a linear n qubit cluster state is prepared. Subsequent entanglement of third-neighbor qubits then results in the desired two-dimensional cluster.

Alternatively, one could create two four-qubit linear cluster states (e.g., qubits 1 to 4 and qubits 5 to 8). These linear graph states could then be converted into box cluster states by local operations and relabeling of some qubits as described in [35]. Thereafter, entangling qubits 4 and 5 and qubits 3 and 6 would result in the same graph as depicted in Fig. 2.

A. Ions confined in individual potential wells

The inhomogeneity of spin-spin couplings in the case of a single harmonic potential can be treated by locating the ions in the individual potential wells created in microstructured traps. In [17] it is shown that by placing each ion in an individual potential well, uniform nearest-neighbor interactions could be achieved. In that scheme, individual harmonic oscillator potentials (characterized by trap frequencies typically of order 1 MHz) confine a linear array of ions such that they are spatially separated by $10\,\mu$m. The relatively small distance between neighboring potential wells is necessary to achieve reasonably large coupling constants J_{nm}.

In this arrangement of trap potentials, nearest-neighbor couplings dominate. Second (third)-neighbor couplings reach values of $\approx 1/6$ ($\approx 1/25$) of the nearest-neighbor couplings (these specific values result from the choice of the two parameters trap frequency and ion separation mentioned above). Because of the small third-neighbor couplings in this arrangement, the general scheme sketched in Fig. 2 is not well suited for cluster state generation. In [17] it was proposed that a 2D cluster state can be created by utilizing nearest- and second-neighbor couplings in separate steps. This scheme would then require appropriate refocusing pulse sequences to eliminate undesired couplings (e.g., third-neighbor couplings).

An alternative scheme using microstructured traps with electrode dimensions of order $10\,\mu$m or smaller is sketched in the following. One may set the potentials of these individual traps such that, at a given time, only ions i and $i+1$ interact. This will be the case, if $\nu_1^j \gg \nu_1^i, \nu_1^{i+1}$ with $j \neq i, i+1$. This choice of the strength of individual potential wells ensures strong suppression of non-nearest-neighbor couplings (below we give a concrete example). Confining the ions in such a trap configuration and applying a magnetic field gradient for a suitable time such that $\int J_{i,i+1} dt = \pi/2$ results in maximal entanglement between ions i and $i+1$. Thus, a linear cluster state can be obtained by subsequently performing this operation on ions 1 through $N-1$. In order to create a $n \times 2$ cluster state, third-neighbors need to be entangled, that is, ions 1 and 4, 3 and 6, 5 and 8. This may be accomplished by first setting ν_1^1 through ν_1^4 to a frequency much lower than the remaining frequencies to enable coupling between ions 1 and 4. Now, ions 1 and 4 are entangled utilizing spin-spin coupling and selective refocusing is used on ions 1 through 4 to undo the unwanted couplings in this quartet of ions, thus realizing the coupling J_{14}. The other third-neighbors are entangled analogously.

In order to check the feasibility of implementing this scheme with currently available ion traps we performed numerical calculations of electrostatic potentials achievable in a typical microstructured trap.

1. *Realization with microstructured traps*

The schemes for generating cluster states outlined above require ion traps with electrode structures at a characteristic length scale of around $10\,\mu$m in order to achieve coupling constants in the kilohertz regime. Even though such structures appear feasible, they imply that the distance between ions and a solid-state surface is of

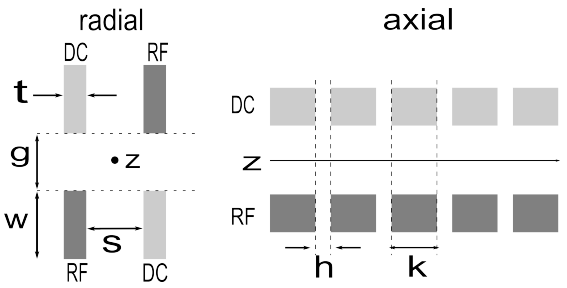

FIG. 3: (Color online) Sketch of the geometry of a segmented ion trap considered for potential simulations. The electrode layers are separated by $s = 350\,\mu$m, while separation in radial direction is $g = 250\,\mu$m. The thickness of the electrodes is $t = 125\,\mu$m, the axial length $k = 100\,\mu$m, and the axial isolation distance is $h = 30\,\mu$m (compare [41]).

the same order of magnitude, which leads to significant heating rates of the ions' secular motion [36, 37, 38]. This, in turn, is likely to impede precise quantum logic operations [39]. On the other hand, in recent experiments strongly reduced heating rates have been observed with ion traps in cryogenic environments [37, 38]. Thus, by sufficiently cooling ion traps, this difficulty that arises with small electrode structures may be overcome.

For many existing microstructured traps typical axial lengths of electrode segments are of order $100\,\mu$m (see Fig. 3), and isolation spacings between electrode segments are typically of order $30\,\mu$m. Such segmented microtraps could serve to create individual harmonic oscillator potentials for each ion. However, with such relatively large trap structures this would lead to large mutual distances between ions and thus to small coupling constants J. This will make it difficult to employ the schemes outlined above for efficient cluster state generation as will be shown now by means of a concrete example.

For numerical simulations we used the parameters of a microtrap that is currently being developed. This trap is a three-layer microstructured segmented trap with two trapping regions. The upper and lower layers both carry electrodes for applying rf and dc electric fields. The middle layer serves as a spacer and contains segments of current-carrying coils that generate a spatially varying magnetic field [40]. We consider a trapping region in our potential simulation with the following geometric parameters of the electrodes: the two electrode layers are separated by the distance $s = 350\,\mu$m and the segmented electrodes are separated in radial direction by a gap $g = 250\,\mu$m. The thickness of the electrodes is $t = 125\,\mu$m, and the axial length of each electrode segment amounts to $k = 100\,\mu$m. For isolation, the electrode segments are divided by a gap of $h = 30\,\mu$m.

We consider 17 segment electrode pairs for the potential simulation. The simulation was created using the *isim* package [41], which is based on boundary-element methods. All coupling constants calculated in this section are done for six ^{171}Yb$^+$ions.

This ion trap is structured such that for each ion an individual potential well may be applied and thus the trap frequencies can be individually set. It is then possible to generate a sequence of single nearest-neighbor couplings with suppressed non-nearest- neighbor couplings. As noted above, setting two neighboring oscillators' frequencies to small values compared to all other's allows selective coupling of a single pair of qubits.

Segment No.	1	2	3	4	5	6	7	8	9
Voltage / V	48	-8	48	0	37.1	18.3	27.4	18.3	36.8
Segment No.	10	11	12	13	14	15	16	17	
Voltage / V	0	48	0	48	0	48	-8	48	

TABLE I: Example for voltage configuration for the microstructured trap described in the text to establish the single coupling J_{23} in a string of six ^{171}Yb$^+$ions while strongly suppressing all other couplings.

Coupling of, for example, only ions number 2 and 3 can be attained by applying the voltage configuration given in Table I to the trap dc electrodes. These voltages result in the simulated potential shown in Fig. 4. A polynomial fit up to second order yields trap frequencies for oscillators 2 and 3 of 0.35 MHz and 0.27 MHz, whereas all other frequencies are between 0.8 and 1.6 MHz. Furthermore, the distance between oscillators 2 and 3 is smaller by a factor of around 2 compared to the other oscillator distances. The nearest-neighbor coupling constants shown in Table II illustrate that J_{23} dominates over all other couplings by 2 orders of magnitude as desired. But due to the large distance between ions of $140\,\mu$m, even this dominating coupling is very small. So segmented microtraps with much smaller axial electrode lengths and isolation spacings (of order $10\,\mu$m) would be required to achieve J couplings in the kilohertz range.

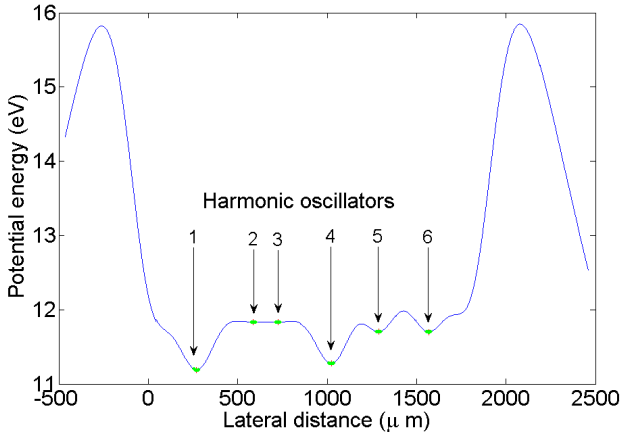

FIG. 4: (Color online) Potential simulation for the voltage configuration shown in Table I. The arrows indicate local potential minima (i.e., the equilibrium position of the respective ion). Oscillators 2 and 3 have small frequencies compared to the other oscillators so that J_{23} is the dominating coupling.

i	$d_{i,i+1}/\mu$m	ν_i/MHz	$J_{i,i+1}$/Hz
1	320	1.65	0.001
2	138	0.35	0.610
3	297	0.27	0.006
4	266	1.16	0.001
5	279	0.83	0.001
6	-	0.98	-

TABLE II: Distances $d_{i,i+1}$ between the individual potential wells $i/i+1$ and axial trap frequencies ν_i determined from polynomial fits up to second order around the potential minima shown in Fig. 4. These parameters clearly lead to the domination of the coupling J_{23} by two orders of magnitude over all other couplings. In this way controlled nearest-neighbor couplings may be implemented without the need for refocusing pulses. To increase J-couplings smaller distances between ions, and therefore smaller electrode structures are required

2. *Periodicity of the time-evolution operator*

The schemes outlined above for preparing a two-dimensional cluster-state are based on the generation of a linear cluster-state of ions and subsequent third-neighbor couplings. These third-neighbor couplings, while undoing the unwanted next-neighbor (NN) couplings, could be accomplished by selective recoupling techniques (compare Sec. II B). However, simultaneous coupling of all qubit pairs would be advantageous. In this section we show that tailoring the time-evolution operator, that is, imposing a suitable periodicity condition by sculpting the J couplings, allows for creation of a cluster state for three qubits, which corresponds to a triangle graph, and the creation of a linear cluster state for four qubits in one time-evolution step.

The general form of the time-evolution operator is:

$$U = \prod_{i<j} \exp(i\Theta_{ij}\sigma_{z,i}\sigma_{z,j}) \ , \tag{4}$$

where $\Theta_{ij} = \int J_{ij}dt$. In order to obtain cluster states by spin-spin coupling, the Θ_{ij} need to take on values of $\frac{\pi}{4}, \frac{\pi}{4}+2\pi, \frac{\pi}{4}+4\pi, ...$, whereas Θ values of $0, 2\pi, 4\pi, ...$ transform the time-development operator into the identity operator. So using periodicity to entangle three qubits requires the following J matrix:

$$\Theta = \int Jdt = \begin{pmatrix} & \frac{\pi}{4}+2k\pi & \frac{\pi}{4} \\ \frac{\pi}{4}+2k\pi & & \frac{\pi}{4}+2k\pi \\ \frac{\pi}{4} & \frac{\pi}{4}+2k\pi & \end{pmatrix} \tag{5}$$

with $k \in \mathbb{N}$. Applying this time evolution to qubits prepared in $|+\rangle^{\otimes 3}$ results in the three-qubit cluster state

$$\begin{aligned} |C_3\rangle &= \exp(i\frac{\pi}{4}(\sigma_{z,1}\sigma_{z,2}+\sigma_{z,1}\sigma_{z,3}+\sigma_{z,2}\sigma_{z,3}))|+\rangle^{\otimes 3} \\ &=_{l.u.} \frac{1}{2}(|000\rangle + |111\rangle) \ . \end{aligned} \tag{6}$$

Here l.u. denotes equivalence up to local unitaries.

One may also utilize the periodicity relation to realize only NN interactions. In this case, the J matrix reads:

$$\Theta = \int Jdt = \begin{pmatrix} & \frac{\pi}{4}+2k_3\pi & 2k_2\pi & 2k_1\pi \\ \frac{\pi}{4}+2k_3\pi & & \frac{\pi}{4}+2k_4\pi & 2k_2\pi \\ 2k_2\pi & \frac{\pi}{4}+2k_4\pi & & \frac{\pi}{4}+2k_3\pi \\ 2k_1\pi & 2k_2\pi & \frac{\pi}{4}+2k_3\pi & \end{pmatrix} \tag{7}$$

with $k_1, k_2, k_3, k_4 \in \mathbb{N}$. The time evolution (4) describes an effective nearest-neighbor interaction, thus generating the linear four-qubit cluster state:

$$\begin{aligned} |C_4\rangle &= \exp(i\frac{\pi}{4}(\sigma_{z,1}\sigma_{z,2}+\sigma_{z,2}\sigma_{z,3}+\sigma_{z,3}\sigma_{z,4}))|+\rangle^{\otimes 4} \\ &=_{l.u.} \frac{1}{2}(|0000\rangle + |0011\rangle + |1100\rangle - |1111\rangle) \ . \end{aligned} \tag{8}$$

Replacing the matrix elements $\Theta_{14} = 2k_1\pi = \Theta_{41}$ in matrix 7 by $\Theta_{14} = 2k_1\pi + \pi/4 = \Theta_{41}$ would allow for generating a 2D cluster state.

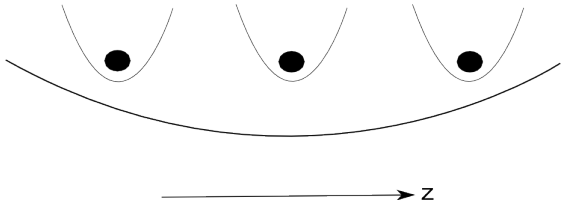

FIG. 5: Locating ions in individual microtraps and superposing a harmonic long-range potential serves to create coupling constants suitable for periodic entanglement.

In the following we show how coupling matrices can be achieved that fulfill the desired periodicity. As before (Sec. II A 1), the ions are placed in individual harmonic oscillator potential wells with adjustable frequencies. Superposing a long range harmonic potential affecting all ions, one more degree of freedom is available (sketched in Fig. 5). So the problem reduces to finding trap frequencies resulting in J couplings that fulfill the periodicity relation. The coupling constants are functions of the ions' equilibrium positions, which can be calculated analytically only for two and three ions. Furthermore, a change in only one trap parameter, say in one trap frequency, affects all couplings simultaneously. So due to the highly non-linear nature of the coupling constants as well as the sensitivity to parameter alterations, finding trap configurations that are suitable for utilizing the periodicity condition becomes increasingly difficult with the number of ions involved. Here we present empirically found parameters.

Consider three Yb^+ ions in individual potential wells superposed by a harmonic long-range potential of frequency $\omega = 2\pi \times 100\,$kHz. Trap frequencies of traps 1 and 3 are $2\pi \times 277\,$kHz. The middle individual trap has frequency $2\pi \times 100\,$kHz (see Figs. 5 and 6). The potential wells are separated by a distance of $20\,\mu$m, and a magnetic field gradient of $100\,$T/m is applied along the trap

axis. These parameters result in the following J matrix:

$$J/(100\text{ Hz}) = \begin{pmatrix} & 7.85 & 0.87 \\ 7.85 & & 7.85 \\ 0.87 & 7.85 & \end{pmatrix} \tag{9}$$

These couplings are useful for cluster state preparation since the periodicity relation is fulfilled:

$$\frac{J_{21}}{J_{31}} = 9.02 \approx \frac{2\pi + \pi/4}{\pi/4} \tag{10}$$

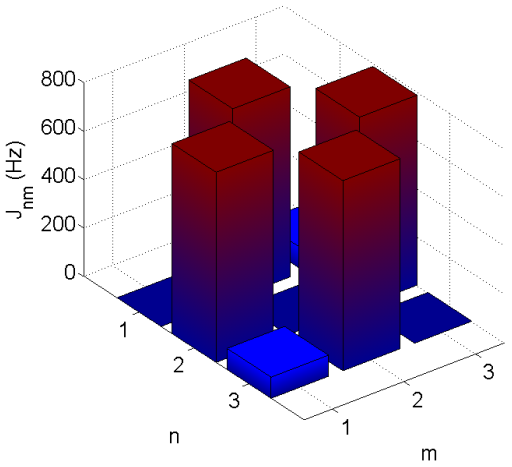

FIG. 6: (Color online) Coupling constants suitable for generating a triangle graph state in one time evolution for three Yb^+ ions in individual potential wells superimposed on a harmonic long-range potential of frequency $\omega = 2\pi \cdot 100$ kHz. Trap frequencies of traps 1 and 3 are $2\pi \cdot 277$ kHz. The middle individual trap has frequency $2\pi \cdot 100$ kHz.

In an analogous fashion, we present parameters useful for generating a four-qubit NN interaction. The four ions are again located in individual traps of frequency $\omega_1 = \omega_4 = 2\pi \times 415$ kHz and $\omega_2 = \omega_3 = 2\pi \times 280$ kHz. A harmonic long-range potential of frequency $\omega = 2\pi \times 239$ kHz is then applied. The individual traps are separated by $5\,\mu$m, and the magnetic-field gradient is again $\frac{\partial B}{\partial z} = 100$ T/m. With these parameters, we obtain the following J matrix:

$$J/(100\text{ Hz}) = \begin{pmatrix} & 4.33 & 2.08 & 1.05 \\ 4.33 & & 4.36 & 2.08 \\ 2.08 & 4.36 & & 4.33 \\ 1.05 & 2.08 & 4.33 & \end{pmatrix} \tag{11}$$

which results in following periodicity relations:

$$\begin{aligned} \frac{J_{32}}{J_{41}} &= 4.15 \approx \frac{4 \cdot 2\pi + \pi/4}{2\pi} \\ \frac{J_{21}}{J_{41}} &= 4.12 \approx \frac{4 \cdot 2\pi + \pi/4}{2\pi} \\ \frac{J_{31}}{J_{41}} &= 1.98 \approx \frac{2 \cdot 2\pi}{2\pi}. \end{aligned} \tag{12}$$

We conclude from the case of three ions that periodic entanglement is in principal possible, but as can be seen from the case of four ions, finding appropriate trap frequencies becomes more and more difficult with higher number of ions due to the non-linearity of the problem. We conjecture that numerical approaches such as genetic algorithms could be efficiently applied to find optimal parameter configurations.

In Sec. II A 1 it was demonstrated that suitable voltage configurations can be found to implement a desired coupling matrix. In order to attain reasonably large coupling constants small electrode structures (of order $10\,\mu$m) are required. For the scheme presented in Sec. II A 2, relying on appropriate periodicity of the time-evolution operator, again small electrode structures are required to be implemented efficiently.

B. Including ion transport for generating cluster states

Now we turn to the description of a different scheme for generating cluster states, which takes advantage of the capabilities of segmented ion traps, even with relatively large electrodes. Segmented ion traps may not only serve for creating an array of linearly arranged potential wells, but also for transporting ions into different trap regions as well as for separation of ions held in a common trap into two distinct traps [24, 25, 26, 27, 28, 29].

Adiabatic ion transport using segmented microtraps has been demonstrated by Rowe et al. [24]. In this experiment a $^9Be^+$ ion was transferred between trap locations 1.2 mm apart in $50\,\mu$s with almost unit efficiency. Furthermore, separation of two ions held initially in a common trap into distinct traps was demonstrated. This was accomplished by using a five electrode configuration. Fast non-adiabatic transport of $^{40}Ca^+$ ions was reported in [29]. The experimental results show a success rate of 99.0(1)% for a transport distance of 2×2mm in a round-trip time of $T = 20\,\mu$s. Application of optimal control theory is planned to achieve lower excitation of vibrational motion in the future.

A $n \times 2$ cluster is prepared using the scheme illustrated in Fig. 2. This generation of cluster states is accomplished in two operational sequences. During the first sequence nearest-neighbor couplings are established that lead to the preparation of a one-dimensional cluster state. The second sequence then establishes couplings between third-neighbor qubits and serves to create a 2D cluster state of eight ions. These two sequences will be detailed in what follows. First, we outline the sequences and state the required time evolution. Then, numerical simulations of the potentials of a microstructured ion trap, which is currently being tested, will serve to illustrate the feasibility of the proposed scheme.

1.6	0	2	0	2	0	2	0	2	0	2	0	2	0	2	0	1.6

TABLE III: Voltage configuration for creating 8 harmonic potential wells such that oscillators 2 to 7 have uniform axial frequencies of 200 kHz. Voltage at electrode pairs 1 and 17 is lower in order to reduce fringe effects.

1. *First sequence: creating a 1D cluster state*

The first sequence itself consists of two steps. During the first time step with duration t_1, pairs of ions, namely ions number 1 and 2, 3 and 4, 5 and 6, 7 and 8 occupy a common trap potential. Switching on the magnetic field gradient for a desired time results in $N/2$ uniform nearest-neighbor couplings:

$$H_{t_1} = -\frac{\hbar}{2} J_{1,2}(\sigma_{z,1}\sigma_{z,2} + \sigma_{z,3}\sigma_{z,4} + \sigma_{z,5}\sigma_{z,6} + \sigma_{z,7}\sigma_{z,8}) \quad (13)$$

The duration t_1 is chosen such that $\int_0^{t_1} J dt = \frac{\pi}{2}$ is fulfilled and the time-evolution operator

$$U_{t_1} = \exp(i\frac{\pi}{4}(\sigma_{z,1}\sigma_{z,2} + \sigma_{z,3}\sigma_{z,4} + \sigma_{z,5}\sigma_{z,6} + \sigma_{z,7}\sigma_{z,8})) \quad (14)$$

is obtained.

At the end of the first time interval, the magnetic-field gradient is turned off (i.e., the spin-spin is zero), and the ions sharing a common trap are separated and transported into potential wells such that ions 2 and 3, 4 and 5, 6 and 7 occupy a common trap. When the ion transport is finished, the magnetic-field gradient is switched on again during time t_2, thus resulting in the other half of NN couplings:

$$U_{t_2} = \exp(i\frac{\pi}{4}(\sigma_{z,2}\sigma_{z,3} + \sigma_{z,4}\sigma_{z,5} + \sigma_{z,6}\sigma_{z,7})) \quad (15)$$

The time evolution during the first sequence described above (i.e., between $t = 0$ and $t = t_2$) requires $N/2$ potential wells of equal axial trap frequency for N ions. We now show that the required axial potential can be realized using the segmented microtrap introduced in Sec. I B. Applying a voltage of 1.6 V to the outermost electrodes, and an alternating series of 2 V and 0 V, respectively, on the remaining dc electrode pairs (Table III), results in harmonic axial potentials of frequency $\omega = 2\pi \times 200$ kHz (compare Fig. 7)

Six of the eight created harmonic oscillators have the same frequency, so that the scheme for preparing a two-dimensional eight-qubit cluster state can be realized with this axial potential. Keeping the pairs of ions 1 and 2 through 7 and 8 in potential wells 2 through 5 for the time t_1 results in the time evolution according to Eq. (14) when the magnetic-field gradient is switched on. Thereafter, the field gradient is deactivated, and the ions are rearranged, such that ions 1 and 8 occupy potential wells 2 and 6 respectively, and the pairs of ions 2 and 3 through 6 and 7 are located in wells 3 through 5. Reactivating the field gradient for a time t_2 leads to the evolution given in Eq. (15), thus creating an eight-qubit linear cluster state.

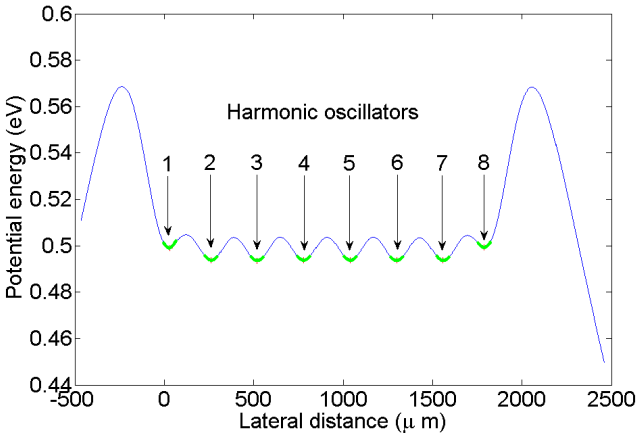

FIG. 7: (Color online) Simulated potential for the voltage configuration shown in Tab.III. Six of eight potential wells have uniform axial frequencies of 200 kHz as well as equidistant axial spacings of 260 μm.

TABLE IV: Distances between the minima of the potential wells in μm for the voltage configuration shown in Tab. III

230	260	260	260	260	259	231

The distances between the minima of the potential wells are shown in Table IV. The characteristic value of the distances between the traps 2 to 7 is simply given by $2\cdot(k+h) = 260\,\mu$m. Deviating values of oscillators 1 and 8 can be explained by fringe effects.

Trap frequencies of $\omega = 2\pi \times 200$ kHz and a magnetic-field gradient of $\partial_z B = 100$ T/m result in coupling constants of ≈ 3 kHz. In Fig. 8 the coupling constants for the time evolution for $0 < t < t_1$ are displayed and Fig. 9 shows the coupling values for $t_1 < t < t_2$. Non-nearest-neighbor couplings are suppressed by 4 orders of magnitude due to the large distance of more than 260 μm between the corresponding ions.

2. *Second sequence: transforming a 1D cluster state into a 2D cluster state*

Now that a linear cluster state has been prepared during the first sequence of operations, qubits 1 and 4, 3 and 6, and 5 and 8 need to be entangled in order to prepare a two-dimensional cluster state during the second sequence. This can be achieved in three steps. In the first step of the second sequence during time interval $t_2 < t < t_3$, qubits 1 through 4 are stored in a common trap, e.g., with trap frequency $\omega = 2\pi \times 200$ kHz, while all other ions occupy single, individual traps with trap distances of 260 μm. Now, applying a magnetic-field gra-

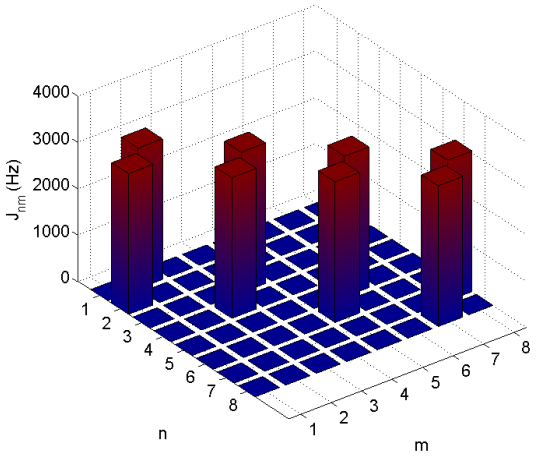

FIG. 8: (Color online) Coupling constants for 8 ions stored in individual harmonic potential wells (shown in Fig. 7). Each potential well is occupied by two ions, yielding uniform NN couplings of 3 kHz between ions number 1 and 2, 3 and 4, etc.. These coupling constants are required for the first time evolution in the first sequence of operations at the end of which a 2D cluster state is obtained. Non-nearest-neighbor couplings are suppressed by four orders of magnitude.

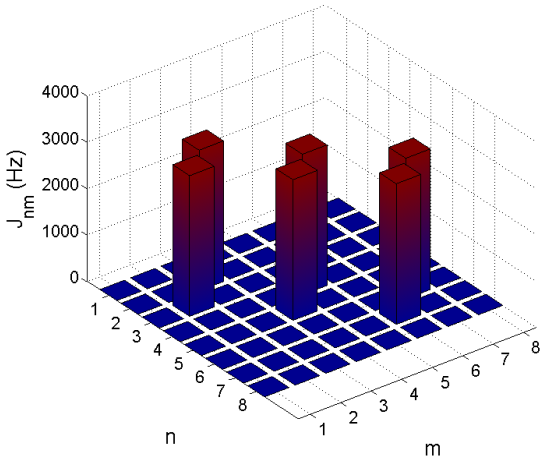

FIG. 9: (Color online) After creating the NN couplings shown in Figure 8, the magnetic field gradient is switched off. Then, ions sharing a common oscillator are separated and transported into four other potential wells, so that ions 2 and 3, 4 and 5 etc. occupy now a common well. Switching on a magnet field gradient of 100 T/m results in uniform NN couplings of 3 kHz again. This completes the second step of the first sequence of operations required for a 2D cluster.

dient of 100 T/m results in a coupling of spins 1 and 4 of $J_{14} = 1.24\,\mathrm{kHz}$ with time- evolution operator

$$U(t_{14}) = \exp(-\frac{i}{2} \sum_{n,m=1;n\leq m}^{4} J_{n,m} t_{14} \sigma_{z,n} \sigma_{z,m}). \quad (16)$$

Other couplings involving qubits 1 to 4 can be canceled by selective recoupling pulse sequences [34]. All couplings regarding qubits 5 to 8 can be neglected during this time interval, since those are approximately 0.5 Hz. The entire time evolution for coupling ions 1 and 4 including pulses to eliminate couplings involving qubits 2 and 3 is thus given by

$$\begin{aligned} U_{t_3} =& U(t_{14}/4)\sigma_{x,2}U(t_{14}/4)\sigma_{x,2}\times \\ & \times \sigma_{x,3}U(t_{14}/4)\sigma_{x,2}U(t_{14}/4)\sigma_{x,2}\sigma_{x,3}, \end{aligned} \quad (17)$$

where $t_{14} = \frac{\pi}{2J_{14}}$ and $\sigma_{x,k}$ denotes the usual Pauli X operator acting on the Hilbert space of qubit k. To see that U_{t_3} implements only the coupling between qubits 1 and 4, it is convenient to think of the two rows as individual sequences. In each of the two sequences, all couplings involving qubit 2 are eliminated, because applying $\sigma_{x,2}$ before and after $U(t_{14}/4)$ adds a minus sign to every $\sigma_{z,2}$ in this time-evolution due to the commutation relation of the Pauli matrices. Analogously, the $\sigma_{x,3}$ at the beginning and end of the second sequence affects nothing but adding a minus sign to all couplings involving qubit 3. In total, all couplings to qubits 2 and 3 differ in their signs for exactly half of the time, and thus they are eliminated. On the other hand, the coupling of qubit 1 to 4 has the same sign during the entire sequence, such that $U_{t_3} = \exp(-i\frac{\pi}{4}\sigma_{z,1}\sigma_{z,4})$.

At the end of time interval t_{14}, the magnetic-field gradient is switched off, and the same procedure is repeated to entangle ions 3 and 6, respectively 5 and 8. Then the ions are arranged in a configuration, such that ions 3 to 6 occupy a common potential well and all other ions are located in separate trap potentials. Switching on the magnetic-field gradient again results in

$$U(t_{36}) = \exp(-\frac{i}{2} \sum_{n,m=3;n\leq m}^{6} J_{n,m} t_{36} \sigma_{z,n} \sigma_{z,m}), \quad (18)$$

and the time evolution including recoupling pulses reads

$$\begin{aligned} U_{t_4} =& U(t_{36}/4)\sigma_{x,4}U(t_{36}/4)\sigma_{x,4}\times \\ & \times \sigma_{x,5}U(t_{36}/4)\sigma_{x,4}U(t_{36}/4)\sigma_{x,4}\sigma_{x,5}, \end{aligned} \quad (19)$$

with $t_{36} = \frac{\pi}{2J_{36}}$. Repeating this procedure for entangling ions 5 and 8, one obtains the following time evolution:

$$\begin{aligned} U_{t_5} =& U(t_{58}/4)\sigma_{x,6}U(t_{58}/4)\sigma_{x,6}\times \\ & \times \sigma_{x,7}U(t_{58}/4)\sigma_{x,6}U(t_{58}/4)\sigma_{x,6}\sigma_{x,7}, \end{aligned} \quad (20)$$

where $t_{58} = \frac{\pi}{2J_{58}}$ and

$$U(t_{58}) = \exp(-\frac{i}{2} \sum_{n,m=5;n\leq m}^{8} J_{n,m} t_{58} \sigma_{z,n} \sigma_{z,m}). \quad (21)$$

The result of this procedure is the cluster state based on the graph shown in Fig. 2:

$$\begin{aligned}|\Psi\rangle =& U_{t_5}U_{t_4}U_{t_3}U_{t_2}U_{t_1}|+\rangle^{\otimes 8} \\ =& \exp(-i\frac{\pi}{4}(\sigma_{z,1}\sigma_{z,4}+\sigma_{z,3}\sigma_{z,6}+ \\ &+\sigma_{z,5}\sigma_{z,8}+\sum_{i=1}^{7}\sigma_{z,i}\sigma_{z,i+1})|+\rangle^{\otimes 8}.\end{aligned} \tag{22}$$

This scheme can be scaled to any $n \times 2$ cluster, which may then serve to simulate a $n \times m$ cluster.

3. Summary of transport scheme for generating 2D cluster states

A summary of the scheme that makes use of transport of ions over small distances is provided in Table V. If we restrict the scheme to adiabatic ion transport, the required time t_T for transport must obey $t_T >> 2\pi/\nu_1$. For $\nu_1 \approx 2\pi \times 200\,\mathrm{kHz}$, we estimate $t_T = 50\,\mu\mathrm{s}$ which is still more than 1 order of magnitude less than the time required for entangling the qubits. The ions need only be linearly transported over distances of the order of the size of two electrode segments; in our concrete example considered above this amounts to a distance of around $200\,\mu\mathrm{m}$.

Adiabatic switching of the magnetic-field gradient would require a time scale of order $t_B >> \frac{2\pi}{\omega}$, if only the qubit states $|0\rangle$ and $|1\rangle$ were present. However, usually other nearby ionic states have to be included in these considerations. For example, in the case of $^{171}\mathrm{Yb}^{+}$ions and choosing $|0\rangle \equiv |S_{1/2}, F = 0\rangle$ and $|1\rangle \equiv |S_{1/2}, F = 1, m_F = 1\rangle$ one would require $t_B >> \frac{2\pi}{\Delta}$ to avoid transitions between Zeeman states, where Δ indicates the Zeeman splitting of the $(S_{1/2},\ F = 1)$ state. In order to avoid zero crossings of the states, while the magnetic-field gradient is changed, a constant offset field is used, e.g., such that $\Delta = 2\pi 10\,\mathrm{MHz}$ without gradient, so that we estimate $t_B \approx 1\,\mu\mathrm{s}$.

During this switching process the qubits' phases are affected due to the spin-spin coupling and the evolution of the Zeeman state. Applying the decoupling scheme described in [34] with appropriate time intervals removes changes in the qubits' phases due to this Zeeman evolution together with the undesired spin-spin couplings as described above.

III. CONCLUSION

We propose methods to generate cluster states of trapped ions confined in state-of-the-art segmented linear ion traps by engineering their spin-spin coupling constants. Based on the idea of simulating a $n \times m$ cluster by a $n \times 2$ cluster within the one-way model of quantum computing, we examined in Sec. II A a method previously suggested [17] to prepare $n \times 2$ clusters, and a novel idea based on creating individual potential wells for each ion. In addition, the superposition of harmonic potentials is discussed in order to engineer J couplings fulfilling suitable periodicity relations to create small cluster states in one time-evolution step. In order to achieve sizeable coupling constants (in the kilohertz range), all these methods require control over local electrostatic potentials with a spatial resolution of the order $10\,\mu\mathrm{m}$ – a typical interion distance in usual Paul traps. Therefore, it is of interest to investigate how suitable a trap with larger electrode structures is for generating 2D cluster states.

In Sec. II B a scheme for preparing $n \times 2$ clusters is described for which larger trap electrode structures (of the order $100\,\mu\mathrm{m}$) are sufficient. Here, $n \times 2$ clusters are prepared by first creating a linear cluster and subsequently enabling third-neighbor couplings. We showed that the generation of the linear cluster state can be accomplished with modern segmented ion traps by locating pairs of two ions in common harmonic oscillators, thus resulting in uniform NN couplings. After separating the ions and subsequently merging them with the other nearest-neighbors, the second half of NN couplings are realized. The required third-neighbor couplings are achieved via selective recoupling techniques.

Common to all schemes described in this paper is that entanglement is achieved solely by controlling dc voltages and currents: no coherent interaction between laser light and trapped ions is required. Refocusing pulses applied to individual ions consist of radio-frequency or microwave radiation depending on the choice of qubit [22, 23, 42, 43].

The method described in Sec. II B is explicitly worked out for the generation of a eight-qubit 2D cluster state. This scheme is also applicable to the generation of $n \times 2$ cluster states where $n = k \times 4$, $k = 2, 3, 4, ...$ The recipe would then be to create in parallel k 2D cluster states of size 4×2. Then in, one additional step, ions at the edges of neighboring 4×2 clusters are entangled. For example, generating a 8×2 cluster proceeds as follows: first create two 2D cluster states of size 4×2, then by combining ions number 7, 8, 9, and 10 in one potential well, simultaneously entangle ion pairs 8/9 and 7/10 to complete a 16-qubit 2D cluster state.

The physical arrangement of a 2D cluster state of size $n \times 2$ is not required to be a linear ion string as was assumed so far. For instance, eight ions could reside in one area of a large 2D trap array [44] and communication between different areas, and thus entanglement, could be achieved by shuttling only the ions at the ends of each ion string.

The spin-spin coupling that is used here does not require cooling of the ion string to its motional ground state. Detailed calculations show that cooling to the Doppler limit is sufficient for suppressing unwanted effects of thermal motion. This is beyond the scope of this paper and will be subject of a separate publication.

Step	Operation
1	Transporting ions 1/2, 3/4, 5/6, 7/8 in common trap potentials
	Entangling ions 1/2, 3/4, 5/6, 7/8
2	Transporting ions 2/3, 4/5, 6/7 in common trap potentials
	Entangling of ions 2/3, 4/5, 6/7
3	Recombination of ions 1 - 4 and 5 - 8
	Entangling ions 1 and 4 using selective recoupling
4	Recombination of ions 3 - 6
	Entangling ions 3 and 6 using selective recoupling
5	Recombination of ions 5 - 8
	Entangling ions 5 and 8 via selective recoupling

TABLE V: Summary of transport scheme for preparing a $n \times 2$ cluster state in a segmented ion trap with magnetic-field gradient of $100\,\mathrm{T/m}$. Steps 1 through 2 serve to create a linear cluster state, while steps 3 through 5 create additional third neighbor couplings that turn the one-dimensional cluster into a two-dimensional cluster. Here, the coupling constants $J_{i,i+1} = 3.0\,\mathrm{kHz}$ for preparation of the linear cluster state which yields the gate times $t_j = \frac{\pi}{2J_{i,i+1}} = 0.52\,\mathrm{ms}$, $j = 1, 2$. In the case of 4 ions sharing a common potential well $J_{1,4}, J_{3,6}, J_{5,8}$ are given by $1.2\,\mathrm{kHz}$ and we have $t_j = \frac{\pi}{2J_{i,i+1}} = 1.3\,\mathrm{ms}$, $j = 3, 4, 5$. The time scale for adiabatically transporting ions is $t_T \gg 2\pi/\nu_1 \approx 5\,\mu\mathrm{s}$. The time scale for adiabatically turning on and off the magnetic field is $t_B \gg 2\pi/\Delta$. When using $^{171}\mathrm{Yb}^+$ions the relevant Δ indicates the Zeeman splitting of the $(S_{1/2}, F = 1)$ state and $2\pi/\Delta$ is typically of order $0.1\,\mu\mathrm{s}$

Acknowledgements

We acknowledge financial support by the STREP Microtrap funded by the European Union, the European Union IP QAP, by the Deutsche Forschungsgemeinschaft, and by secunet AG.

[1] H. J. Briegel and R. Raussendorf, Phys. Rev. Lett. **86**, 910 (2001).
[2] R. Raussendorf and H. Briegel, Quantum Inf. Comput. **6**, 443 (2002).
[3] R. Raussendorf, D. E. Browne, and H. J. Briegel, Phys. Rev. A **68**, 022312 (2003).
[4] T. Rudolph and J. W. Pan, Focus Issue on Measurement-Based Quantum Information Processing, special issue of New J. Phys. **9** (2007).
[5] R. Raussendorf, D. E. Browne, and H. J. Briegel, J. Mod. Opt. **49**, 1299 (2002).
[6] D. M. Greenberger, M. A. Horne, and A. Zeilinger, in *Bell's Theorem, Quantum Theory, and Conceptions of the Universe* edited by M. Kafatos (Kluwer, Dordrecht, 1989), pp. 69–72.
[7] W. Dür, Phys. Rev. Lett. **92**, 180403 (2004).
[8] M. A. Nielsen, Rep. Math. Phys. **57**, 147 (2006).
[9] O. Mandel, M. Greiner, A. Widera, T. Rom, T. W. Hänsch, and I. Bloch, Nature (London) **425**, 937 (2003).
[10] P. Walther, K. Resch, T. Rudolph, E. Schenck, H. Weinfurter, V. Vedral, M. Aspelmeyer, and A. Zeilinger, Nature (London) **434**, 169 (2005).
[11] M. S. Tame, R. Prevedel, M. Paternostro, P. Bohi, M. S. Kim, and A. Zeilinger, Phys. Rev. Lett. **98**, 140501 (2007).
[12] C.-Y. Lu, X.-Q. Zhou, O. Guehne, W.-B. Gao, J. Zhang, Z.-S. Yuan, A. Goebel, T. Yang, and J.-W. Pan, Nat. Phys. **3**, 91 (2007).
[13] H. S. Park, J. Cho, J. Y. Lee, D.-H. Lee, and S.-K. Choi, Opt. Express **15**, 17960 (2007).
[14] P. A. Ivanov, N. V. Vitanov, and M. B. Plenio, Phys. Rev. A **78**, 012323 (2008).
[15] K. Mølmer and A. Sørensen, Phys. Rev. Lett. **82**, 1835 (1999).
[16] A. Sørensen and K. Mølmer, Phys. Rev. A **62**, 022311 (2000).
[17] D. Mc Hugh, Ph.D. thesis, National University of Ireland Maynooth 2005.
[18] D. Mc Hugh and J. Twamley, Phys. Rev. A **71**, 012315 (2005).
[19] M. G. Raizen, J. M. Gilligan, J. C. Bergquist, W. M. Itano, and D. J. Wineland, Phys. Rev. A **45**, 6493 (1992).
[20] J. P. Schiffer, Phys. Rev. Lett. **70**, 818 (1993).
[21] D. H. E. Dubin, Phys. Rev. Lett. **71**, 2753 (1993).
[22] C. Wunderlich, in *Laser Physics at the Limit*, edited by H. Figger, D. Meschede, C. Zimmermann (Springer Verlag, Berlin, 2002) pp. 261–271.
[23] C. Wunderlich and C. Balzer, Adv. At. Mol. Opt. Phys. **49**, 295 (2003).
[24] M. A. Rowe, A. Ben-Kish, B. DeMarco, D. Leibrandt, V. Meyer, J. Beall, J. Britton, J. Hughes, W. M. Itano, B. Jelenkovic, C. Langer, T. Rosenband, D. J. Wineland, Quantum Inf. Comput. **2**, 257 (2002).
[25] W. K. Hensinger, S. Olmschenk, D. Stick, D. Hucul, M. Yeo, M. Acton, L. Deslauriers, C. Monroe, and J. Rabchuk, Appl. Phys. Lett. **88**, 034101 (2006).
[26] S. Schulz, U. Poschinger, K. Singer, and F. Schmidt-Kaler, Fortschr. Phys. **54**, 648 (2006).
[27] R. Reichle, D. Leibfried, R. Blakestad, J. Britton, J. Jost, E. Knill, C. Langer, R. Ozeri, S. Seidelin, and D. Wineland, Fortschr. Phys. **54**, 666 (2006).
[28] D. Hucul, M. Yeo, W. K. Hensinger, J. Rabchuk, S. Olmschenk, and C. Monroe, Quantum Inf. Comput. **8**, 0501 (2008).

[29] G. Huber, T. Deuschle, W. Schnitzler, R. Reichle, K. Singer, and F. Schmidt-Kaler, New J. Phys. **10**, 013004 (2008).
[30] D. Porras and J. I. Cirac, Phys. Rev. Lett. **92**, 207901 (2004).
[31] S. Stahl, F. Galve, J. Alonso, S. Djekic, W. Quint, T. Valenzuela, J. Verd, M. Vogel, and G. Werth, Eur. Phys. J. D **32**, 139 (2005).
[32] G. Ciaramicoli, F. Galve, I. Marzoli, and P. Tombesi, Phys. Rev. A **72**, 042323 (2005).
[33] G. Ciaramicoli, I. Marzoli, and P. Tombesi, Phys. Rev. A **75**, 032348 (2007).
[34] D. W. Leung, I. L. Chuang, F. Yamaguchi, and Y. Yamamoto, Phys. Rev. A **61**, 042310 (2000).
[35] G. Gilbert, M. Hamrick, and Y. S. Weinstein, Phys. Rev. A **73**, 064303 (2006).
[36] Q. A. Turchette, D. Kielpinski, B. E. King, D. Leibfried, D. M. Meekhof, C. J. Myatt, M. A. Rowe, C. A. Sackett, C. S. Wood, W. M. Itano, et al., Phys. Rev. A **61**, 063418 (2000).
[37] L. Deslauriers, S. Olmschenk, D. Stick, W. K. Hensinger, J. Sterk, and C. Monroe, Phys. Rev. Lett. **97**, 103007 (2006).
[38] J. Labaziewicz, Y. Ge, P. Antohi, D. Leibrandt, K. R. Brown, and I. L. Chuang, Phys. Rev. Lett. **100**, 013001 (2008).
[39] D. J. Wineland, C. Monroe, W. M. Itano, D. Leibfried, B. E. King, and D. M. Meekhof, J. Res. Natl Inst. Stand. Technol. **103**, 259 (1998).
[40] D. Brüser, M. Johanning, and C. Wunderlich, (unpublished).
[41] S. A. Schulz, U. Poschinger, F. Ziesel, and F. Schmidt-Kaler, New J. Phys. **10**, 045007 (2008).
[42] F. Mintert and C. Wunderlich, Phys. Rev. Lett. **87**, 257904 (2001); F. Mintert and C. Wunderlich, *ibid.* **91**, 029902 (2003)
[43] M. Johanning, A. Braun, N. Timoney, V. Elman, W. Neuhauser, and C. Wunderlich, Phys. Rev. Lett. **102**, 073004 (2009).
[44] D. Kielpinski, C. Monroe, and D. J. Wineland, Nature **417**, 709 (2002).